

Synchrotron-radiation photoemission study of CdS/CuInSe₂ heterojunction formation

Art J. Nelson and Steve Gebhard

Solar Energy Research Institute, 1617 Cole Boulevard, Golden, Colorado 80401

Angus Rockett

*Department of Materials Science and Engineering, University of Illinois at Urbana-Champaign,
1304 West Green Street, Urbana, Illinois 61801*

Elio Colavita

Department of Physics, University of Calabria, I-87036 Arcavacata di Rende, Cosenza, Italy

Mike Engelhardt and Hartmut Höchst

Synchrotron Radiation Center, University of Wisconsin-Madison, 3731 Schneider Drive, Stoughton, Wisconsin 53589-3097

(Received 30 April 1990)

Synchrotron-radiation soft-x-ray photoemission spectroscopy was used to investigate the development of the electronic structure at the CdS/CuInSe₂ heterojunction interface. CdS overlayers were deposited in steps on single-crystal *p*- and *n*-type CuInSe₂ at 250°C. Results indicate that the CdS grows in registry with the substrate, initially in a two-dimensional growth mode followed by three-dimensional island growth as is corroborated by reflection high-energy electron-diffraction analysis. Photoemission measurements were acquired after each growth in order to observe changes in the valence-band electronic structure as well as changes in the In 4*d*, Se 3*d*, Cd 4*d*, and S 2*p* core lines. The results were used to correlate the interface chemistry with the electronic structure at these interfaces and to directly determine the CdS/CuInSe₂ heterojunction valence-band discontinuity and the consequent heterojunction band diagram. These results show that the Katnani-Margaritondo method is unreliable in determining offsets for heterojunctions where significant Fermi-level pinning may occur and where the local structure and chemistry of the interface depends strongly on the specific heterojunction.

I. INTRODUCTION

The ternary $A^{\text{I}}B^{\text{III}}X_2^{\text{VI}}$ chalcopyrite semiconductor CuInSe₂ exhibits superior performance as an absorber in heterojunction solar cells¹⁻³ and has potential applications for light-emitting diodes⁴ and various nonlinear devices.⁵ Polycrystalline thin-film⁶ and single-crystal⁷ photovoltaic devices with efficiencies exceeding 12% have been reported. The theoretical electronic structure of CuInSe₂ has been determined⁸ but experimental data is still somewhat limited.^{9,10} In addition, theoretical,^{11,12} and experimental¹³⁻¹⁵ data on the formation of the CdS/CuInSe₂ heterojunction is limited and inconclusive. Thus, important gaps exist in our knowledge of the electronic properties of this technologically important heterojunction.

This paper presents and discusses the results of a synchrotron-radiation soft-x-ray photoemission investigation of CdS/CuInSe₂ heterojunction formation. CdS overlayers were deposited in steps on single-crystal *p*- and *n*-type CuInSe₂ at 250°C. Photoemission spectra were obtained before and after each growth in order to observe the development of the electronic structure at the heterojunction interface.

II. EXPERIMENT

The CuInSe₂ crystals (*p* and *n* type) were sliced from a boule which was prepared by the gradient freezing method.¹⁶ Carrier concentrations were $5.3 \times 10^{16} \text{ cm}^{-3}$ for the *n*-type crystal and $3 \times 10^{17} \text{ cm}^{-3}$ for the *p*-type crystal. The samples were mechanically polished and then etched in a solution formulated from 10 g KBr in 100 ml H₂O (+0.2 ml Br₂) for 30 s prior to insertion into the analysis chamber. Quantitative compositional analysis was performed with electron-microprobe analysis (EMPA) using x-ray wavelength-dispersive spectroscopy which determined that the samples were stoichiometric CuInSe₂.

A single liquid-nitrogen-shrouded boron nitride effusion cell was the source of the deposited CdS films. Deposition rates were monitored with a calibrated water-cooled quartz crystal thickness monitor and showed the typical Arrhenius behavior (the deposition rate is linear versus the reciprocal of the absolute source temperature). The observed linear growth rate indicates that the effusion cell releases stoichiometric amounts of CdS in a certain temperature range (650–750°C) and can be used as a molecular-beam source for growth.

Photoemission experiments were performed using a "Grasshopper" monochromator on the 1-GeV storage ring (Aladdin) at the University of Wisconsin Synchrotron Radiation Center. The photoemitted electrons were analyzed using a hemispherical sector analyzer with 1.5° angular acceptance mounted on a two-axis goniometer. Photoemission spectra were taken in an energy range $h\nu = 70\text{--}130$ eV. The combined energy resolution of the monochromator and the analyzer was $\Delta E \approx 0.1$ eV. All spectra were measured at normal emission with a photon angle of incidence of $\theta_c = 45^\circ$. Prior to analysis, each crystal surface was cleaned *in situ* by sputtering with 1-keV Ar ions in order to obtain a clean valence-band spectra. Sputter-induced damage was removed by annealing for ≈ 2 min at 500°C .

III. RESULTS AND DISCUSSION

The reflection high-energy electron-diffraction (RHEED) patterns of the polished and etched *p*- and *n*-type CuInSe_2 crystals showed bright three-dimensional diffraction plots along a ring characteristic of oriented single-crystal CuInSe_2 . After the crystal surfaces were cleaned *in situ* by sputter etching with 1 keV Ar ions, the RHEED patterns consisted of rings indicating a random amorphous surface as one might expect after sputtering. Only when the sputter etched crystals were annealed at 500°C did the rings disappear and the original spots reappear. This is consistent with previous work¹⁷ which concluded that CuInSe_2 crystals could be sputtered with up to 1.5 keV Ar ions and annealed at 500°C without changing the surface composition. However, EMPA indicated that both CuInSe_2 crystals lost 0.5 at. % Se from the bulk due to the 500°C anneal in vacuum. Surface sensitive *in situ* core-level spectroscopy confirmed that the CuInSe_2 surfaces were atomically clean. Following this surface preparation, CdS was deposited at 250°C on both *p*- and *n*-type CuInSe_2 . The RHEED patterns of the CdS overlayers were similar to the virgin substrates indicating that the CdS grows in registry with the substrate.

In order to fully characterize the CuInSe_2 substrate prior to CdS growth, the valence-band (VB) spectra of the *p*- and *n*-type CuInSe_2 were acquired with several photon energies with the typical *n*-type VB spectra series presented in Fig. 1 for discussion. Comparison of the experimental VB structure with the theoretically predicted band structure⁸ as determined by a self-consistent potential-variation mixed-basis approach shows the following.

(i) The upper valence band ($T_{4v}-\Gamma_{4v}-N_{1v}$, where T and N are high-symmetry points in a body-centered tetragonal Brillouin zone) has a calculated width of 4.8 eV and consists of a mixture of Se $4p$ and Cu $3d$ orbitals which, due to the relative proximity of the Se $4p$ and Cu $3d$ orbital energies, interact. The observed upper valence band appears as a two-peak structure corresponding to the two branches of the Cu d bands. The calculated peak density of states is near $E_v - 3.3$ eV which is higher than the observed value of $E_v - 2.4$ eV by 0.9 eV [E_v is the valence-band maximum (VBM) and is determined from the linear extrapolation of the leading edge as outlined

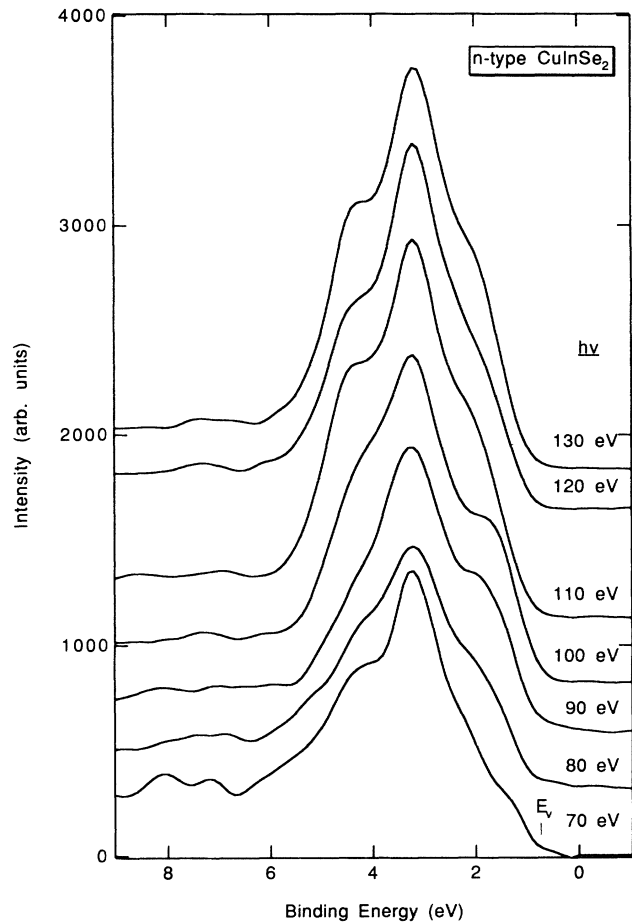


FIG. 1. Normal emission valence-band spectra of *n*-type CuInSe_2 following etch and *in situ* sputter cleaning acquired in the energy range $h\nu = 70\text{--}130$ eV.

below]. The observed upper valence-band structures for both single-crystal *n*- and *p*-type CuInSe_2 are thus in reasonably good agreement with theory. The observed emission above E_v originates from the convolution of the lifetime-broadened emission with the finite energy resolution of the electron analyzer and monochromator.^{18,19}

(ii) The In—Se band ($T_{5v}-\Gamma_{2v}-N_{1v}$) has its peak density of states near $E_v - 6.0$ eV and a calculated maximum width of 0.7 eV. This band is only observed at the lower photon energies due to variations in the corresponding photoionization cross sections and is observed at $E_v - 6.3$ eV for both *p*- and *n*-type CuInSe_2 .

(iii) At yet higher binding energies, theory predicts a Se $4s$ band ($T_{5v}-\Gamma_{1v}-N_{1v}$) between $E_v - 12.8$ eV to $E_v - 13.2$ eV. This band was not observed due to its low photoionization cross section in the photon energy range used for this study.

(iv) The calculated binding energy of the In $4d$ core-level peak relative to the VBM is at 16.9 eV. Figure 2 displays the In $4d$ peak as a function of CdS coverage. At zero coverage, this peak is observed at $E_v - 17.4$ eV for both *p*- and *n*-type CuInSe_2 , which is in agreement with literature values.^{9,10}

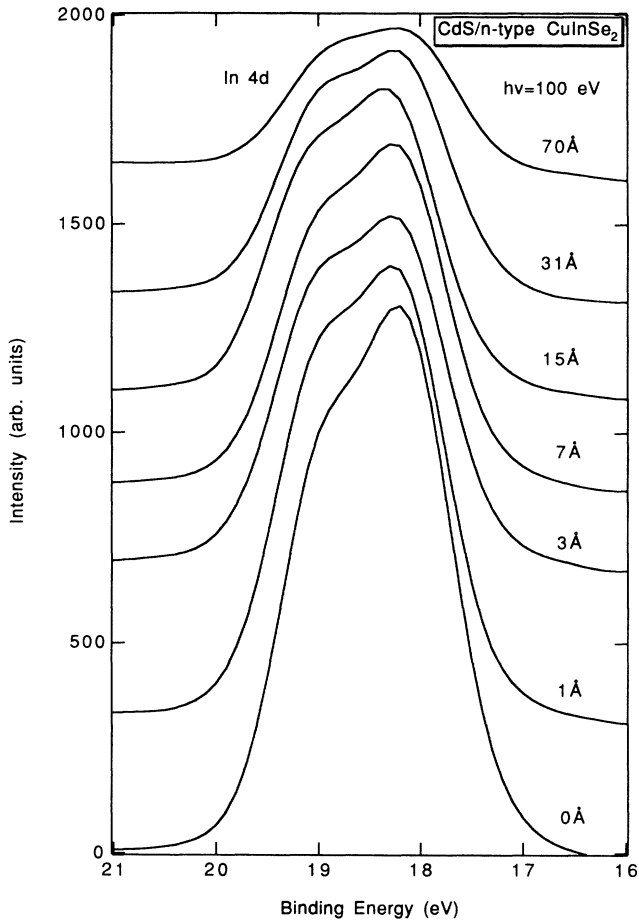


FIG. 2. Characteristic In 4d core-level emission for CuInSe₂ as a function of the effective CdS coverage.

Figure 3 shows a plot of the normalized intensity of the In 4d core-level emission as a function of the nominal thickness of the CdS overlayer film (from Fig. 2) representative of growth on both the *p*- and *n*-type CuInSe₂. The nominal thickness necessary for one monolayer of CdS would be equal to 3.36 Å (5.82 Å/√3). The kinetic energy of the photoemitted electrons is ≈ 74 eV which is at the minimum of the universal escape depth curve. For homogeneous coverage of the substrate without diffusion, one expects the substrate core-level intensity to decrease exponentially (linear on a semi-ln plot) for a two-dimensional layer-by-layer growth mode. Additionally, a small amount of In outdiffusion would account for the observed In signal intensity and would not lead to a significant deviation from exponential attenuation. The lines fit to the experimental data points show two regions of growth as evidenced by the two different slopes. This knee in the substrate attenuation curve at a film thickness of 10–15 Å indicates a change from the initial two-dimensional growth mode to a mixed three-dimensional island growth mode (Stranski-Krastanov growth) which is corroborated by the corresponding RHEED images. The initial layer-by-layer growth can be

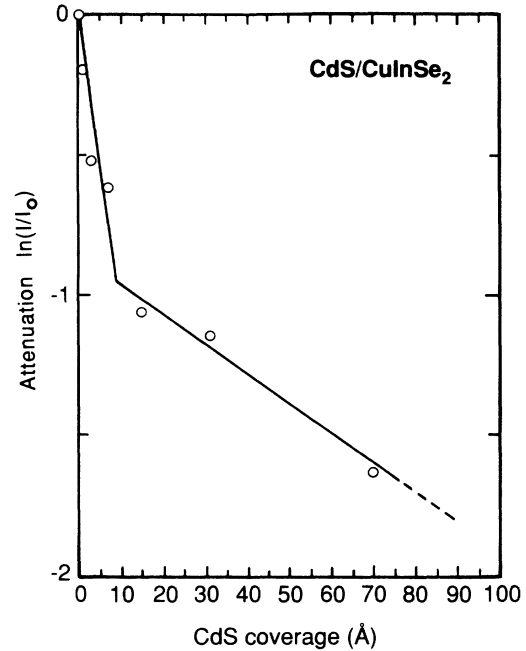


FIG. 3. Normalized substrate In 4d core-level emission intensity as a function of nominal CdS overlayer thickness.

understood by noting that the lattice constants for the two materials are similar (5.82 Å for cubic CdS and 5.78 Å for CuInSe₂) thus allowing two-dimensional growth. The transition to three-dimensional growth may indicate that the CdS becomes strained thus making three-dimensional growth more energetically favorable.

Figure 4 shows the normal emission valence-band spectra of the CdS/CuInSe₂ interface as a function of the effective CdS coverage for the *n*-type crystal. The evolution of the VBM shown in these figures is a direct indication of the evolution of the electronic structure leading to the CdS/CuInSe₂ heterojunction formation. The position of the VBM (E_v) for each coverage is determined from the linear extrapolation of the leading edge. Linear extrapolation of the leading edge of VB emission is somewhat arbitrary and can account for errors in the determination of the VBM. However, the band-mapping analysis^{18,19} necessary for the precise determination of E_v was impractical for this investigation and would not significantly affect the value of the valence-band discontinuity. Therefore, in the case of the *n*-type CuInSe₂, E_v shifts by 0.3 ± 0.1 eV on going from clear *n*-type CuInSe₂ to the 70 Å CdS overlayer spectrum. Similarly, E_v shifts by 0.3 ± 0.1 eV on going from clean *p*-type CuInSe₂ to the 300 Å CdS overlayer spectrum. These shifts do not directly correspond to the valence-band discontinuity ΔE_v between CuInSe₂ and CdS since the position of the substrate valence-band edge at the interface is modified by adatom-induced changes in the band bending.²⁰ Therefore, in order to determine ΔE_v , one needs an independent estimate of the band-bending potential for both *p*- and *n*-type substrates. Specifically, three quantities are necessary to determine ΔE_v for this heterojunc-

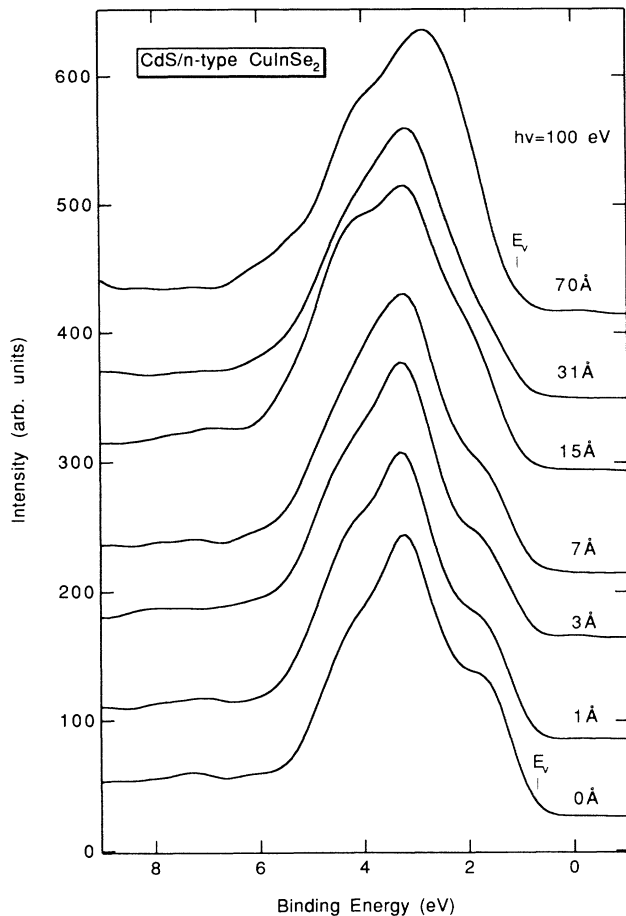


FIG. 4. Normal emission valence-band spectra of the CdS/CuInSe₂ interface as a function of the effective CdS coverage for the *n*-type crystals.

tion, two of which are the core-level to valence-band maximum energy separation for each constituent of the heterojunction. The third quantity is the core-level binding energy difference ΔE_{cl} for a core level on each side of the heterojunction referenced to E_F .²¹

Band bending potentials can be determined by monitoring the corresponding shifts of the substrate core-level photoemission peaks as long as contributions due to chemical shifts can be separated. It has been determined that for most binary semiconductors, the anion core levels are severely affected by adatom-induced changes in the chemical shift and therefore cannot be used to estimate band bending variations.²⁰ However, it has been determined that the cation core levels are not affected by changes in the chemical shift and thus their adatom induced shifts can be used directly to determine band bending variations.

The In 4*d* core-level emission for *n*- and *p*-type CuInSe₂ as a function of the effective CdS coverage (Fig. 2) depicts the evolution of the In 4*d* peak during the formation of the CdS/CuInSe₂ interface. The peak position at zero coverage is $E_v - 17.4$ eV and shifts to $E_v - 17.5$ eV at the lower coverages (1, 3, and 7 Å). This shift reflects the adatom-induced changes in the substrate band bend-

ing. At total coverage, the peak position is $E_v - 17.1$ eV. Thus, the first quantity needed to determine the valence-band discontinuity, specifically $E_{In\ 4d} - E_v$ in the CuInSe₂, is 17.4 eV.

The representative Cd 4*d* core-level emission for *n*- and *p*-type CuInSe₂ as a function of the effective CdS coverage is presented in Fig. 5. For the lower CdS coverages, the peak position is $E_v - 10.5$ eV and shifts to $E_v - 10.1$ eV at the higher coverages. Thus, the last two quantities necessary for the determination of the valence-band discontinuity are extracted, specifically, $E_{Cd\ 4d} - E_v$ in CdS is 10.1 eV and $E_{In\ 4d} - E_{Cd\ 4d}$ across the heterojunction is 7.0 eV (referenced to E_F).

Using the results of these three measurements it is clear that the valence-band discontinuity ΔE_v is 0.3 eV for the CdS/(*n*-type CuInSe₂) heterojunction. Similarly, the valence-band discontinuity for the CdS/(*p*-type CuInSe₂) heterojunction is 0.3 eV. Combining these results with $E_g(\text{CuInSe}_2) = 1.04$ eV and $E_g(\text{CdS}) = 2.42$ eV, one may determine the conduction-band discontinuity ΔE_c to be 1.08 eV for an abrupt CdS/(*n*-type CuInSe₂) or CdS/(*p*-type CuInSe₂) heterojunction. These results are summarized schematically in Fig. 6 for the *n*-type CuInSe₂ heterojunction. The experimental data show no

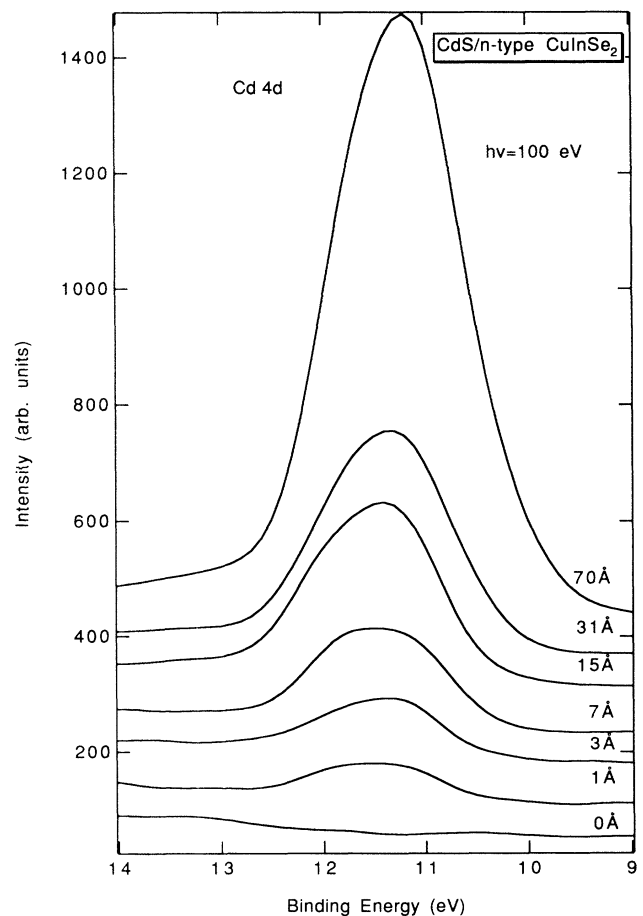


FIG. 5. Characteristic Cd 4*d* core-level emission for CuInSe₂ as a function of the effective CdS coverage.

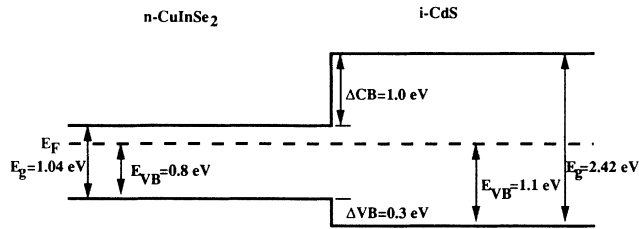


FIG. 6. Schematic of the experimentally determined band lineup across the CdS/CuInSe₂ heterojunction.

band bending for either case due to (i) 3–5 Å probe depth and (ii) the low carrier concentration since the width of the space-charge region is inversely proportional to the square root of the carrier concentration.

These CdS/CuInSe₂ heterojunctions are most commonly used for solar-cell applications. It is clear that no solar cell could operate with weakly doped CdS, not only because of the series resistance which would result in the CdS, but also because of the presence of a substantial barrier to conduction of either carrier type from the CuInSe₂ to the CdS (Fig. 6). Normally, solar cells are fabricated with heavily In-doped CdS which is strongly *n* type. Furthermore, there is a possibility that In will diffuse across the heterojunction further enhancing the conductivity of the CdS. In this case, the Fermi level in the CdS would rise to near the conduction-band edge and the CuInSe₂ band edges would equalize to match the Fermi levels across the junction. This would lead to strong band bending near the heterojunction. If the CdS is much more heavily doped than the CuInSe₂, most of the band bending will occur in the CuInSe₂. The amount of band bending will exceed the energy gap of the CuInSe₂ and thus a thin two-dimensional electron gas will develop near the heterojunction due to diffusion of electrons out of the *n*⁺-type CdS as shown schematically in Fig. 7(a). This electron gas will act as a metal and will be present for any type or level of doping in the CuInSe₂ but would be smallest in heavily *n*-type material.

This model only applies to single-crystal CuInSe₂/CdS heterojunctions but may aid in explaining several previously unexplained observations concerning CdS/CuInSe₂ heterojunctions and solar cells, in general. Specifically, the apparent lack of interface-dominated recombination of minority carriers,²² the presence of buried homojunctions in the CuInSe₂ as observed by electron-beam-induced conductivity (EBIC) (Ref. 23), and the broad range of CuInSe₂ compositions around stoichiometry for which good solar cells can be fabricated.²⁴ All of these observations are consistent with the presence of an induced homojunction. The presence of a two-dimensional electron gas in the CuInSe₂ near the heterojunction will produce an essentially metallic contact which will be relatively insensitive to the type of epitaxy or quality of the CdS/CuInSe₂ interface. When the CuInSe₂ is substoichiometric it tends to be weakly *p* type. Thus, the formation of an electron gas near the heterojunction will invert the local carrier population in the CuInSe₂, forming an induced homojunction. The depth of this homo-

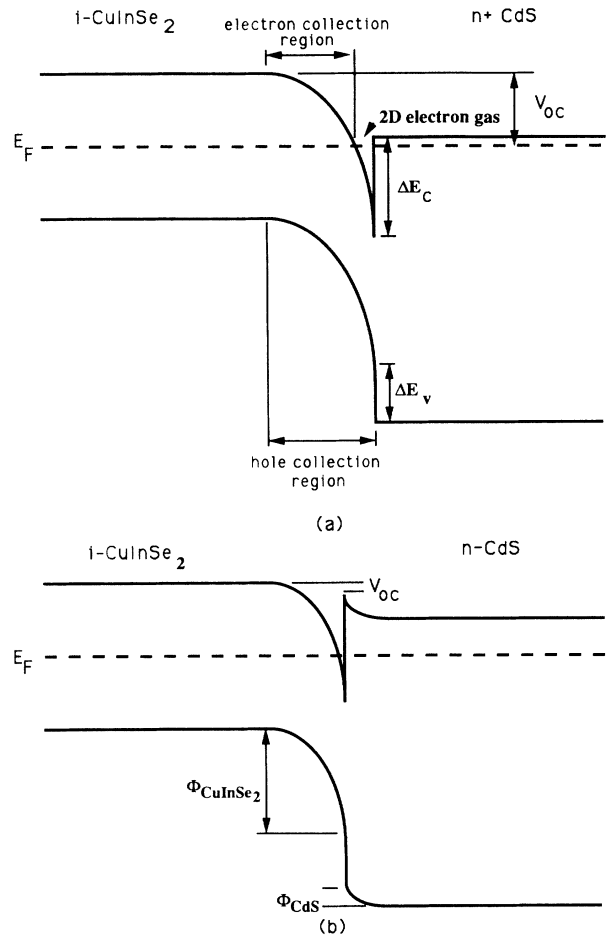


FIG. 7. CdS/CuInSe₂ heterojunction models for (a) band bending in the CuInSe₂ and (b) with band bending in the CdS.

junction will depend on the doping level of the CuInSe₂ and will increase with the resistivity of the material. In fact, such an induced homojunction would appear even for *n*⁻-type CuInSe₂, as observed.

In the case of thin films, as the compositions of the CuInSe₂ becomes In-rich, the films are observed to be weakly *n* type with carrier concentrations in the 10¹⁵ cm⁻³ range up to ≈2% excess In. Near stoichiometry, the carrier concentration changes to *p* type and rises rapidly. It is reasonable to assume that the Fermi level lies near the center of the band gap for both In-rich and stoichiometric material, falling toward *E_v* as the material becomes Cu-rich. As long as band bending occurs primarily in the CuInSe₂, the open circuit voltage (*V_{oc}*) of the solar cell will be determined by (*E_c* – *E_F*) in the CuInSe₂ [Fig. 7(a)]. The open circuit voltage will drop significantly if band bending occurs in the CdS as shown schematically in Fig. 7(b).

It has been previously suggested²⁵ that the band-edge discontinuity should occur primarily in the valence band. This conclusion is based on the temperature dependence of the solar-cell behavior and on photoemission data for CdS/Si (Ref. 26) and CuInSe₂/Si (Ref. 10) heterojunctions and applying a generalized empirical method.²⁰

However, this method is unreliable in heterojunctions where significant Fermi-level pinning may occur in one of the materials at the interface and where the local structure and chemistry of the interface depends strongly on the heterojunction in question. On the basis of the above arguments showing that the observed band-edge discontinuities are consistent with observed heterojunction behavior, we conclude that the majority of the band-edge discontinuity actually occurs in the conduction-band edge for single-crystal CuInSe₂/CdS heterostructures.

IV. CONCLUSIONS

We have presented the results of a synchrotron-radiation soft-x-ray photoemission investigation of the CdS/CuInSe₂ heterojunction interface. The valence-band discontinuity for this heterojunction has been experimentally determined and a heterojunction band diagram for

CdS on single-crystal *n*- and *p*-type CuInSe₂ has been constructed thus explaining numerous factors affecting the ultimate performance of these single-crystal devices. The results also show that the Katnani-Margaritondo method is unreliable in determining offsets for heterojunctions where significant Fermi-level pinning may occur and where the local structure and chemistry of the interface depends strongly on the specific heterojunction. Future experiments will include performing a similar growth procedure using CuInSe₂ thin films.

ACKNOWLEDGMENTS

The authors would like to thank Fouad Abou-Elfotouh for supplying the CuInSe₂ crystals grown at the University of Salford and L. L. Kazmerski, Tim Coutts, Alex Zunger, and Manuel Cardona for helpful discussions. This work was supported by the U.S. Department of Energy under Contract No. DE-AC02-83CH10093.

-
- ¹S. Wagner, J. L. Shay, P. Migliorato, and H. M. Kasper, *Appl. Phys. Lett.* **25**, 434 (1975).
- ²L. L. Kazmerski, F. R. White, and G. K. Morgan, *Appl. Phys. Lett.* **29**, 268 (1976).
- ³R. A. Mickelsen and W. S. Chen, in *Proceedings of the 16th IEEE Photovoltaic Specialists Conference* (IEEE, New York, 1982), p. 781.
- ⁴N. Yamamoto, *Jpn. J. Appl. Phys.* **19**, 45 (1980).
- ⁵B. R. Pamplin, T. Kiyosawa, and K. Masumoto, *Prog. Cryst. Growth Character* **1**, 331 (1979).
- ⁶K. Mitchell, C. Eberspacher, J. Ermer, and D. Pier, in *Proceedings of the 20th IEEE Photovoltaic Specialists Conference, Las Vegas* (IEEE, New York, 1988), p. 1256.
- ⁷J. L. Shay, S. Wagner, and H. M. Kasper, *Appl. Phys. Lett.* **27**, 89 (1975).
- ⁸J. E. Jaffe and Alex Zunger, *Phys. Rev. B* **28**, 5822 (1983).
- ⁹J. C. Rife, R. N. Dexter, P. M. Bridenbaugh, and B. W. Veal, *Phys. Rev. B* **16**, 4491 (1977).
- ¹⁰M. Turowski, G. Margaritondo, M. K. Kelly, and R. D. Tomlinson, *Phys. Rev. B* **31**, 1022 (1985).
- ¹¹Allen Rothwarf, in *Proceedings of the 16th IEEE Photovoltaic Specialists Conference* (IEEE, New York, 1982), p. 791.
- ¹²J. F. Wager, O. Jamjoun, and L. L. Kazmerski, *Solar Cells* **9**, 159 (1983).
- ¹³L. L. Kazmerski, O. Jamjoun, P. J. Ireland, R. A. Mickelsen, and W. S. Chen, *J. Vac. Sci. Technol.* **21**, 486 (1982).
- ¹⁴M. Turowski, M. K. Kelly, G. Margaritondo, and R. D. Tomlinson, *Appl. Phys. Lett.* **44**, 768 (1984).
- ¹⁵P. Zurcher, A. J. Nelson, P. Johnson, G. J. Lapeyre, and L. L. Kazmerski, in *Proceedings of the 19th IEEE Photovoltaic Specialists Conference, New Orleans* (IEEE, New York, 1987), p. 955.
- ¹⁶R. K. Tomlinson, *Solar Cells*, **16**, 17 (1986).
- ¹⁷P. Corvini, A. Kahn, and S. Wagner, *J. Appl. Phys.* **57**, 2967 (1985).
- ¹⁸D. W. Niles and H. Hochst, *Phys. Rev. B* **39**, 7769 (1989).
- ¹⁹H. Hochst, D. W. Niles, and I. Hernandez-Calderon, *Phys. Rev. B* **40**, 8370 (1989).
- ²⁰A. D. Katnani and G. Margaritondo, *Phys. Rev. B* **28**, 1944 (1983).
- ²¹E. A. Kraut, R. W. Grant, J. R. Waldrop, and S. P. Kowalczyk, *Phys. Rev. B* **28**, 1965 (1983).
- ²²M. Roy, S. Damaskinos and J. E. Phillips, in *Proceedings of the 20th IEEE Photovoltaic Specialists Conference, Las Vegas* (IEEE, New York, 1988), p. 1618.
- ²³R. J. Matson, R. Noufi, R. K. Ahrenkiel, R. C. Powell, and D. Cahen, *Solar Cells* **16**, 495 (1986).
- ²⁴R. E. Rocheleau, J. D. Meakin, and R. W. Birkmire, in *Proceedings of the 19th IEEE Photovoltaic Specialists Conference, New Orleans* (IEEE, New York, 1987), p. 972.
- ²⁵G. B. Turner, R. J. Schwartz and J. L. Gray, in *Proceedings of the 20th IEEE Photovoltaic Specialists Conference, Las Vegas* (IEEE, New York, 1988), p. 1457.
- ²⁶A. D. Katnani and G. Margaritondo, *J. Appl. Phys.* **54**, 2522 (1983).